Small-Angle Neutron Scattering of Poly(styrene)/Poly(acrylic acid–ethyl acrylate) Copolymers: The Effect of the Degree of Hydrolysis of the Poly(acrylic acid–ethyl acrylate) Block

Mark A. Crichton, Surita R. Bhatia

Department of Chemical Engineering, University of Massachusetts, Amherst, Massachusetts 01003-9303

Received 10 October 2003; accepted 9 December 2003
DOI 10.1002/app.20429
Published online in Wiley InterScience (www.interscience.wiley.com).

ABSTRACT: We report the results of systems based on polystyrene-poly(ethyl acrylate) (PEA) diblocks, which self-assemble in aqueous solutions to form spherical micelles. Previous work has shown that the rheological properties of these solutions, in particular the gel–liquid transition, can be tuned through the use of a simple hydrolysis reaction to convert PEA to poly(acrylic acid) (PAA). We studied the effect of the extent of hydrolysis on the self-assembly and micellar interactions. Small-angle neutron scattering (SANS) spectra were fit with a variety of models to determine the micelle structure. As more PEA was converted to PAA (i.e., as the corona became more charged and more hydrophilic), the micellar aggregation number decreased, analogous to observations of other polymeric micelles. This effect could impact the gel–liquid transition and rheology in this system and in similar micellar block copolymer gels. Finally, our SANS spectra qualitatively agreed with predictions for attractive colloidal glasses, confirming the idea that the elasticity of these gels arises from the jamming of micelles. J Appl Polym Sci 93: 490–497, 2004

Key words: diblock copolymers; polyelectrolytes; polystyrene; gelation; neutron scattering

INTRODUCTION

Diblock polyelectrolytes consisting of a charged hydrophilic block and a hydrophobic block are of interest for a variety of industrial applications, including viscosity modifiers for personal care products and drilling fluids for oil-field applications. Such systems also exhibit fascinating morphological behavior, as demonstrated by Eisenberg and coworkers.[1] One such system is polystyrene (PS)/poly(acrylic acid) (PAA), which can display morphologies including spherical micelles, single and multilamellar vesicles, and bicontinuous rods. The morphology can be controlled by variation of the ionic strength, solvent, or degree of polymerization of the diblocks.[1,2] These copolymers tend to self-assemble at low solution concentrations. Fluorescence studies on the critical micelle concentration of PS/PAA diblocks have yielded values in the range 10^{-5} to 10^{-8} *M*, depending on the molecular weight of the copolymer.[3,4]

Groenewegen and coworkers used small-angle neutron scattering (SANS) to examine the spherical micelles of PS/PAA in aqueous solutions, focusing on the micelle structure and counterion distribution as a function of ionic strength.[5,6] Their results show that the structure of the PS core was not sensitive to either the ionic strength or polymer concentration. However, the size of the corona and extension of the PAA chains was highly dependent on ionic strength, with fully ionized chains being nearly completely stretched.[6] Studies using tetramethylammonium counterions in salt-free solutions demonstrated that nearly all of the counterions in these micelles are trapped in the corona layer or bound to the polyelectrolyte block.[6] On the basis of these results, PS/PAA systems with a low aggregation number could be considered almost electroneutral, although the authors noted that even a small fraction of free charge could cause a substantial net charge in systems with large aggregation numbers.[6]

In addition to their versatility with respect to solution morphology and self-assembly, block polyelectrolyte solutions often have interesting rheological behavior that is important in many of the end applications mentioned previously. For example, Tsitsilianis and Iliopoulos showed that PS/PAA/PS triblocks

Correspondence to: S.R. Bhatia (sbhatia@ecs.umass.edu).
Contract grant sponsor: Rhodia Complex Fluids Laboratory.
Contract grant sponsor: Office of Basic Energy Sciences, U.S. Department of Energy; contract grant number: W-31-109-ENG-38.

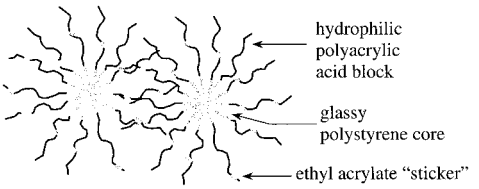

Figure 1 PS/P(AA–EA) micelles associated via ethyl acrylate stickers.

form strong gels at very low polymer concentrations.[7] These gels are analogous to those formed by nonionic telechelic associative polymers, with a networked solution structure. However, these systems also have some rheological characteristics that are similar to chemically crosslinked gels.[7]

We recently investigated diblock polyelectrolyte gels with tunable rheological properties.[8,9] These systems were prepared from polystyrene/poly(ethyl acrylate) (PEA) diblocks. PEA can be partially converted to PAA by a base catalyzed hydrolysis reaction.[9] The extent of the hydrolysis reaction (f) is directly related to the fraction of ethyl acrylate groups along the backbone ($z = 1 - f$) These polymers self-assemble in aqueous solutions to form spherical micelles where the core is comprised of the short PS block and the corona consists of the poly(acrylic acid–ethyl-acrylate) [P(AA–EA)] block (Fig. 1).

The concentration at which gelation occurs and the elastic modulus and viscosity are strong functions of f.[8,9] It is thought that the hydrophobic ethyl acrylate groups act as molecular "stickers" between micelles, causing attractive intermicellar associations that lead to gel formation. However, scaling polymer concentration on the hydrodynamic radius from dynamic light scattering yields effective micellar volume fractions greater than 0.6 for the gels.[10] This indicates that the elasticity is due to crowding of micelles rather than the formation of an attractive network structure.[10] Thus, the gel structure is expected to be analogous to an attractive colloidal glass.

The degree to which the unhydrolyzed ethyl acrylate groups increase their intermicellar attraction is unclear, despite the supporting evidence from rheological studies. In addition, it is unknown whether the ethyl acrylate groups affect the micellar size and aggregation number. The latter effect could also impact the gel–liquid transition, particularly if gel formation occurs via the crowding or jamming of the micelles.[10] To gain insight into such effects, SANS studies were performed on micellar solutions of PS/P(AA–EA) with various f values. The spectra were fit to determine the micelle structure and interaction strength.

EXPERIMENTAL

The diblock polymer was supplied by Rhodia, Inc. (Cranbury, NJ), as PS/PEA with a number-average molecular weight of 2000/19,468 g/mol as determined by GPC.[11] A synthetic technique used by Rhodia (macromolecular design via the interchange of xanthates, or MADIX) resulted in a polydispersity of approximately 2.0 for both both blocks; the details of this technique are given elsewhere.[11–13] The polymer was supplied as an aqueous suspension of latex particles of approximately 40 wt %. The hydrolysis reaction was run with 10 wt % polymer in water at 90°C. When the polymer solution reached 90°C, 2M NaOH aqueous solution was added dropwise. The amount of 2M NaOH added was dependent on the desired degree of hydrolysis. The reaction mixture was then held at 90°C for 24 h. The final degree of hydrolysis was determined with 200-MHz ^{1}H-NMR. After hydrolysis, the polymer was dialyzed with regenerated cellulose membranes with a molecular weight cutoff of 6000–8000 (SpectraPor 1, Spectrum Laboratories, Rancho Dominguez, CA) against an aqueous NaOH solution at pH 10 for about 1 week. This was done to remove impurities and normalize the charge density along the polymer backbone.

SANS measurements were performed on a small-angle diffractometer at the Intense Pulsed Neutron Source (IPNS) located at Argonne National Laboratory, Argonne, IL. We prepared samples for SANS by dissolving freeze-dried polymer in D_2O (Cambridge Isotope Laboratories, Andover, MA) and stirring for several days at 80°C. This was above the glass-transition temperature of low-molecular-weight PS, which facilitated the formation of equilibrium structures.[14] The calculated scattering length densities are shown in Table I. The scattering length density, $\rho_b = \rho b/MN_{AV}$, where N_{AV} is Avagadro's number, b is the scattering length density, ρ is the density, and M is the monomer molecular weight. Spectra were obtained at 25°C for two different polymer concentrations, 0.5 and 4.0 wt %. Quartz sample cells with path lengths of 1 and 2 mm were used for the concentrated and dilute samples, respectively. Spectra were collected for 1–4 h, depending on the sample concentration and contrast. Deuterated water was used to quantify the solvent scattering, which was subsequently subtracted off from the spectra. Incoherent scattering was estimated from the signal at high momentum vector, q, and was also subtracted from the data. The q range covered in these experiments was $0.005\ \text{Å}^{-1} < q < 0.7\ \text{Å}^{-1}$.

TABLE I
ρ_b Values of All of the Components

Component	ρ_b (10^{-6} Å^{-2})
PEA	0.8446
PS	1.2186
D_2O	6.3722
PAA, sodium salt	4.2698

Data analysis

The scattered intensity [$I(q)$] of a monodisperse system can be expressed as the product of the form factor [$F(q)$] and the structure factor [$S(q)$]:

$$I(q) = N(\Delta\rho_b)^2 F(q) S(q) \tag{1}$$

where N is the number density of micelles and $\Delta\rho_b$ is the difference in the scattering length density.

Form factor models

We utilized four different models: a monodisperse spherical $F(q)$, a polydisperse spherical $F(q)$, a core–corona micellar $F(q)$, and a copolymer micelle model proposed by Förster and coworkers.[15,16] $F(q)$ for monodisperse spheres is given by[17]

$$F(q) = \frac{9(\sin qR - qR\cos qR)^2}{(qR)^6} \tag{2}$$

This model only contains one parameter, R the sphere radius (R). We interpret R as the radius of the micelle. The polydisperse hard sphere $F(q)$ includes a parameter to account for the width of the sphere size distribution; assuming a Gaussian size distribution and integrating over the radial coordinate, r, yields

$$F(q) = \int_0^\infty \frac{9}{\sqrt{2\pi\sigma}} e^{-(r-R)^2/2\sigma^2} \frac{(\sin qr - qr\cos qr)^2}{(qr)^6} dr \tag{3}$$

This two-parameter model includes R, the average sphere radius, and the standard deviation of the sphere size distribution (σ). As we did previously, we interpret R and σ characteristic of the micelle size distribution. With this interpretation of R, the micelle aggregation number (N_{agg}) can be calculated as

$$N_{agg} = \frac{4\pi}{3} \frac{R^3}{V_{PS/PAA}} \tag{4}$$

where $V_{\mathrm{PS/PAA}}$ is the volume of the polymer chain.

The core–corona model is widely used to fit the form factor of polymeric micelles, such as poly(ethylene oxide) (PEO)/poly(propylene oxide) (PPO) systems.[18,19] This model accounts for the presence of solvent in the micelle core and brush. Because the PS micelle core was glassy in our system, we assumed that the core completely excludes water.[14] With this assumption, the core–corona model reduces to

$$F(q)(\Delta\rho_b)^2 = \left\{ \left(\frac{4\pi R_1^3}{3}\right)(\rho_{b,PS} - \rho_{b,c}) \left[\frac{3J_1(x_1)}{x_1}\right] + \left(\frac{4\pi R_2^3}{3}\right)(\rho_{b,c} - \rho_{b,c}) \left[\frac{3J_1(x_2)}{x_2}\right] \right\} \tag{5}$$

where R_1 and R_2 are the radii of the micelle core and the entire micelle, respectively; $\rho_{b,\mathrm{PS}}$, $\rho_{b,c}$, and $\rho_{b,\mathrm{s}}$ are the scattering length densities of PS, the corona, and D_2O, respectively; and $J_1(x)$ is the first-order spherical Bessel function

$$J_1(x) = \frac{\sin x - x\cos x}{x^2} \tag{6}$$

where $x_1 = qR_1$ and $x_2 = qR_2$. $\rho_{b,\mathrm{c}}$ can be expressed as

$$\rho_{b,c} = \alpha\rho_{b,P(AA-EA)} + (1 - \alpha)\rho_{b,s} \tag{7}$$

where α is the fraction of P(AA–EA) in the corona. Recall that the chains comprising the corona contain both acrylic acid and ethyl acrylate units; hence, $\rho_{b,\mathrm{P(AA/EA)}}$ is the average scattering length density weighted by z.

R_1, R_2 and α are not independent; they are related through N_{agg}.[19] We can express the aggregation number as

$$N_{agg} = \frac{4\pi R_1^3}{3 V_{PS}} \tag{8}$$

where V_{PS} is the volume of the PS block. Then, the fraction of P(AA/EA) in the corona is[19]

$$\alpha = \frac{3N_{agg}V_{P(AA-EA)}}{4\pi(R_2^3 - R_1^3)} \tag{9}$$

where $V_{P(AA-EA)}$ is the volume of the $P(AA\text{-}EA)$ block.

Thus, with the assumption that there is no water in the PS core, the core–corona model also reduces to a two-parameter model. We chose to fit R_1 and R_2; we could subsequently calculate N_{agg} and α if desired.

A copolymer micelle for factor proposed by Förster and coworkers was also used. This model is based on a scattering length density profile that is constant through the micelle core and decays through the corona. The parameters of this model are the core and corona radii, R_1 and R_2; ρ_{int}, the scattering length density at the core/corona interface; and δ, a parameter that characterizes the corona chain statistics. The full details of this model can be found elsewhere.[15,16]

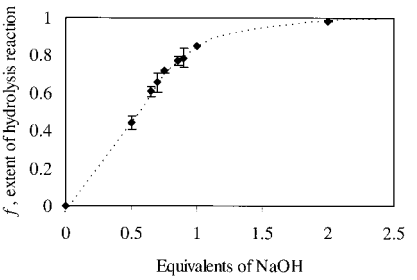

Figure 2 f versus the amount of NaOH used in hydrolysis reaction. The dotted line is a guide for the eye.

Structure factor

We chose to use an adhesive hard sphere (AHS) potential to model $S(q)$.[20,21] The use of such a model for $S(q)$ is fairly standard in the analysis of SANS data from polymeric micelles.[22–24] The AHS structure factor is given by[20,21]

$$S(q) = \frac{1}{A^2 + B^2} \tag{10a}$$

$$k = 2qR_{HS} \tag{10b}$$

$$A = 1 + 12\phi\left(\gamma\frac{\sin\kappa - \kappa\cos\kappa}{\kappa^3} + \xi\frac{1-\cos\kappa}{\kappa^2} - \frac{\lambda}{12}\frac{\sin\kappa}{\kappa}\right) \tag{10c}$$

$$B = 12\phi\left(\gamma\frac{\frac{\kappa^2}{2} - \kappa\sin\kappa + 1 - \cos\kappa}{\kappa^3} + \xi\frac{\kappa - \sin\kappa}{\kappa^2} - \frac{\lambda}{12}\frac{1-\cos\kappa}{\kappa}\right) \tag{10d}$$

The fitted parameters in this model are R_{HS}, the radius of interaction; τ, the "stickiness;" and ϕ, the volume fraction. The parameters λ, γ, and ξ are defined as follows:

$$\lambda = \min\left\{6\left[\frac{\tau}{\phi} + \frac{1}{(1-\phi)}\right] \pm \left(36\left[\frac{\tau}{\phi} + \frac{1}{(1-\phi)}\right]\right)^{1/2}\right\} \tag{11a}$$

$$\mu = \lambda\phi(1-\phi) \tag{11b}$$

$$\gamma = \frac{1 + 2\phi - \mu}{(1-\phi)^2} \tag{11c}$$

$$\xi = \frac{-3\phi + \mu}{2(1-\phi)^2} \tag{11d}$$

Relating ϕ to RHS can reduce the number of fitting parameters in this model, which will be discussed later. The total number of parameters used to fit $I(q)$ then depends on the specific $F(q)$ model chosen. Finally, eq. (1) is strictly correct only for monodisperse systems. We incorporate polydispersity into $S(q)$ with the method of Huang and coworkers, who defined a polydispersity correction factor (ζ) as[25]

$$S'(q) = 1 + \zeta(q)[S(q) - 1] \tag{12}$$

$$\zeta(q) = \frac{\left|\int_0^\infty \frac{9}{\sqrt{2\pi\sigma}} e^{-(R-R_{ave})/2\sigma^2} \frac{(\sin qR - qR\cos qR)}{(qR)^3} dR\right|^2}{\left|\int_0^\infty \frac{9}{\sqrt{2\pi\sigma}} e^{-(R-R_{ave})/2\sigma^2} \frac{(\sin qR - qR\cos qR)^2}{(qR)^6} dR\right|} \tag{13}$$

The intensity is then defined as

$$I(q) = N(\Delta\rho)^2 F(q) S'(q) \tag{14}$$

In fitting our data, however, we found that this effect was minimal and fit with eq. (1), and eqs. (13) and (15) yielded nearly equivalent results.

One potential problem with the adhesive hard sphere model is that it does not allow for compression of the spheres (physically corresponding to brush overlap). Accounting for this effect would be equiva-

TABLE II
Characteristics of Copolymers After the Hydrolysis Reactions

NaOH (equiv)	f	z	Total molecular weight	$\rho_{b,P(AA-EA)}$ (10^{-6}Å^{-2})	$V_{P(AA-EA)}$(Å^3)
0.50	0.44	0.56	18,970	2.359	28,728
0.65	0.61	0.39	18,020	2.934	26,582
0.70	0.65	0.34	17,760	3.092	25,995
0.75	0.72	0.28	17,421	3.297	25,228
0.90	0.79	0.21	17,026	3.537	24,475
2.00	0.97	0.03	15,926	4.181	24,334

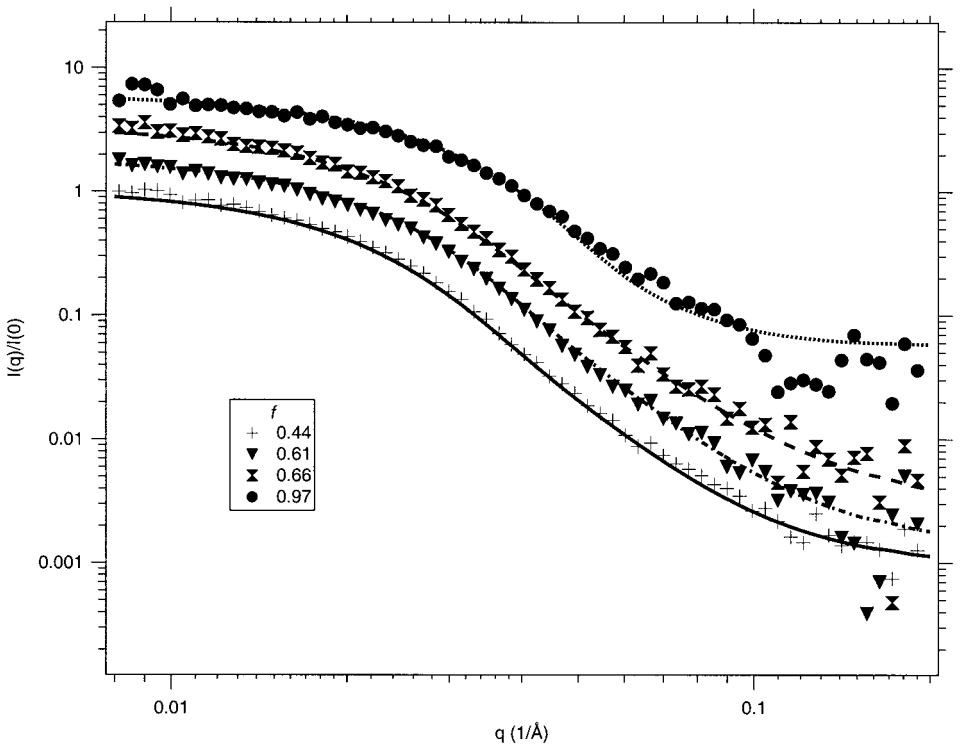

Figure 3 Intensity versus the scattering vector for dilute samples at different extents of hydrolysis. The solid lines are fits to the $F(q)$ for the polydisperse spheres.

lent to the use of a potential with a softer repulsive component. It is unclear whether or not this will be a problem for the PS/P(AA–EA) systems. We expected the repulsive interaction between micelles to be fairly hard; however, as we show later, the AHS model failed to capture some of the behavior at low q for our systems.

RESULTS AND DISCUSSION

Hydrolysis of the diblocks

The hydrolysis reaction was carried out with 0.5–2.0 equiv of NaOH. ^{1}H-NMR analysis of these samples yielded an f value between 0.44 and 0.97, corresponding to fractions of ethyl acrylate (z) between 0.56 and 0.03. The relationship between the equivalents of NaOH used and f is shown in Figure 2. The calculated values for total number-average molecular weight, $\rho_{b,P(AA-EA)}$, and $V_{P(AA-EA)}$ for all of samples are given in Table II.

Dilute solutions: Form factor fits

Figure 3 shows the experimental data for the 0.5 wt % polymer solutions, normalized to unity at low q and offset for clarity. Although intermicellar interactions may have been present in these systems, no correlation peak was observed in the data; thus, we fit these spectra with only the form factor. The lines shown are fits to the polydisperse sphere model [eq. (3)]. For clarity, fits with the other form factor models are not shown. The parameters from the four form factor models are listed in Table III. Note the similarity of the values for the monodisperse sphere fit, the polydis-

TABLE III
Parameters from $F(q)$ Fits to Dilute Samples

Monodisperse sphere		Core–corona			Polydisperse sphere		Copolymer micelle		
f	R(Å)	R_1(Å)	R_2(Å)	α	R (Å)	σ (Å)	R_1(Å)	R_2(Å)	δ
0.44	86.5 ± 0.2	39.6 ± 0.3	87.5 ± 0.2	0.1281	107.5 ± 0.5	27.0 ± 0.3	84.0 ± 0.1	339.3 ± 1.0	0.7 ± 0.005
0.61	80.8 ± 0.2	36.1 ± 0.6	82.6 ± 0.4	0.0807	98.9 ± 0.6	24.9 ± 0.4	78.8 ± 0.6	—	—
0.66	79.2 ± 0.2	27.9 ± 1.0	84.0 ± 0.4	0.0625	99.1 ± 0.8	26.5 ± 0.5	76.9 ± 0.1	317.4 ± 0.4	0.7 ± 0.007
0.97	65.4 ± 0.4	31.2 ± 22.4	67.0 ± 3.5	0.0362	76.1 ± 18.9	16.6 ± 41.3	63.2 ± 0.3	416.2 ± 8.4	0.7 ± 0.02

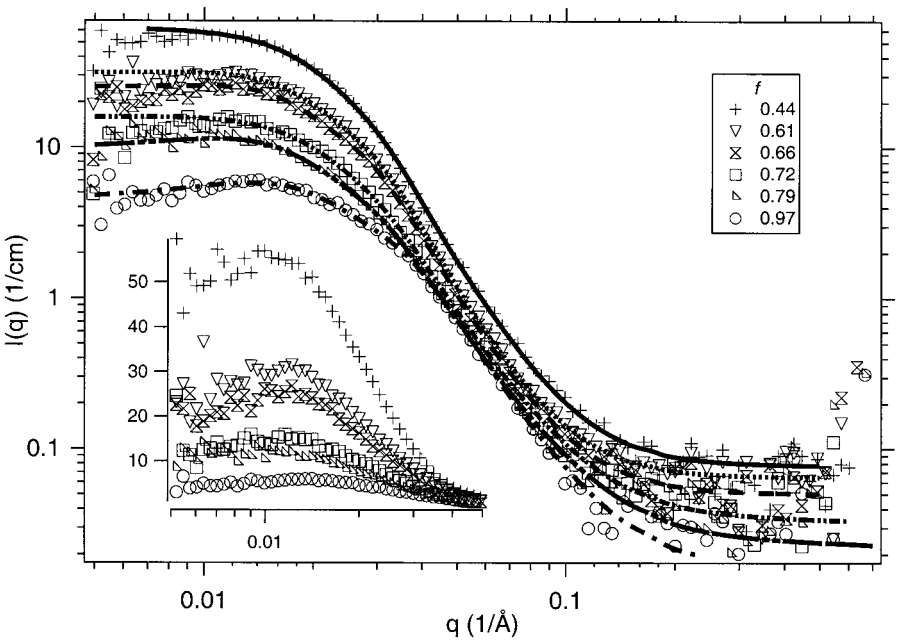

Figure 4 Intensity versus $S(q)$ for concentrated samples at different extents of hydrolysis. The lines are fits with a polydisperse sphere $F(q)$ and an AHS $S(q)$.

perse sphere fit, the micelle radius (R_2) from the core–corona model fit, and the core radius (R_1) from the copolymer micelle fit. The similarity between these four radii, along with the lack of features in the mid-q range of our SANS data, suggested that it was only reasonable to extract one characteristic radius from the spectra and that there was not enough detail in the SANS data to justify the use of more complex form factor models, for example, the copolymer micelle model. This could be due to the low contrast between the core and corona, which did not yield enough signal to fully elucidate the corona structure. This may have been the cause of the large values of R_2 obtained from the copolymer micelle fit. Thus, for our analysis of concentrated systems, the polydisperse sphere form factor was used. The data fit the polydisperse form factor well, yielding an average core radius of 70–100 Å and a polydispersity of 20–25% (σ = 17–27). The core radius decreased with increasing f, which agreed with the trend in the concentrated data, described later.

Concentrated solutions: AHS structure factor fits

On the basis of our SANS fits for the dilute solutions, we chose to model the SANS spectra for the concentrated systems with a polydisperse form factor [eq. (13)] and an AHS structure factor [eqs. (10) and (11)]. To reduce the number of fitted parameters, we recognized that parameters ϕ and R_{HS} are not independent; they are related through the number density of scatterers (N):

$$\phi = \frac{4\pi}{3} R_{HS}^3 N \tag{15}$$

N is related to the number density of micelles by the following expression:

$$N = \frac{cN_{AV}}{MW_{PS/P(AA-EA)} N_{agg}} \tag{16}$$

where c is the concentration of the polymer in solution, $MW_{PS/P(AA–EA)}$ is the molecular weight of the polymer, and N_{AV} is Avogadro's number. Substituting eqs. (4) and (17) into eq. (16) we obtain

$$\phi = \left(\frac{R_{HS}}{R}\right)^3 \frac{cN_{AV}V_{PS/P(AA-EA)}}{MW_{PS/P(AA-EA)}} \tag{17}$$

Fitting the data with the AHS structure factor and polydisperse form factor thus required four parameters: σ, R, R_{HS}, and τ.

All of the concentrated samples formed strong gels. Figure 4 shows the curve fits for the 4.0 wt % systems. A peak corresponding to the intermicellar distance was observed at $q \approx 0.015$ Å^{-1} for all of the samples, which did not change position but got sharper and more intense as f decreased. Thus, localization was stronger in systems with more ethyl acrylate groups (lower values of f). In addition, none of the spectra showed evidence of long-range order; the micelles were arranged in a disordered manner, as opposed to the cubic ordered displayed by several micellar PPO/

TABLE IV
Parameters from Fits to Concentrated Samples

f	Polymer molecular weight	R (Å)	N_{agg}	τ	σ (Å)
0.44	18,970	100.4 ± 0.3	148	0.015 ± 0.006	24.5 ± 0.2
0.61	18,020	94.1 ± 0.3	131	0.020 ± 0.008	22.6 ± 0.2
0.66	17,760	93.5 ± 0.4	132	0.037 ± 0.008	22.9 ± 0.2
0.72	17,421	93.0 ± 0.5	133	—	25.3 ± 0.3
0.79	17,026	89.6 ± 0.6	123	—	24.8 ± 0.4
0.97	15,926	71.7 ± 0.5	63	—	19.2 ± 0.4

PEO/PPO gels.[26,27] These results were in qualitative agreement with predictions from coupling theories of attractive colloidal glasses, which predict a disordered structure with stronger localization of particles as the strength of attraction increases.[28]

Table IV summarizes the parameters from the AHS fit, with the aggregation number calculated with eq. (4). For systems with no value of τ listed in Table IV, the data was well fit by a structure factor with $\tau = 0$. The R values calculated agreed well with the results from the form factor data with the polydisperse sphere model. The aggregation number increased as f decreased or, alternatively, as z increased. There are three possible explanations for this trend. First, the effective size of the corona chains could have increased as f increased due to the increasing charge density. This could have resulted in a decrease in N_{agg} because the spherical configuration could not pack as many corona chains into the micelle. Second, we postulated that the hydrolysis reaction did not cause uniform hydrolysis of the PEA block, leaving regions of unhydrolyzed ethyl acrylate concentrated near the PS block. This, in turn, made the apparent size of the polystyrene core larger due to the similarity of the scattering length densities of PS and PEA, leading to a larger value for N_{agg}. Although such a scenario is possible, we did not have any other evidence that supported this picture. Finally, we could attribute this effect to the increasing hydrophobicity of the corona as f decreased. In general, this effect promotes assembly and causes an increase in the aggregation number. Similar effects have been seen in the micelles of PPO/PEO/PPO and poly(butylene oxide)/PEO, where the aggregation number increased with an increase in the hydrophobic nature of the polymer.[29]

This decrease in N_{agg} with increasing f corresponded to a decrease in the micelle size. As mentioned previously, the gel–liquid transition in these systems depended strongly on f, with the critical polymer concentration for gelation shifting to higher concentrations as f increased. If gel formation occurs through jamming or crowding of the micelles, as some evidence suggests,[10] this trend is consistent with a decrease in the micelle size, as we observed via SANS.

CONCLUSIONS

We investigated the assembly of block polyelectrolyte micelles in which the fraction of hydrophilic groups in the corona chain, f, could be easily varied via hydrolysis. Our dilute and concentrated SANS data showed that N_{agg} decreased as f increased. This was likely due to an increase in the charge density of the corona chains, although the decrease in the corona hydrophobicity or unhydrolyzed ethyl acetate units near the PS core could also have been the cause. The micelle size also decreased as f increased, which was consistent with the shift in the gel–liquid transition to higher polymer concentrations for higher values of f.[8]

Finally, in fitting the spectra from concentrated systems, we found that τ was not very sensitive to the value of f. This suggested that the AHS model might not be suitable to describe the micelle–micelle interactions. This was further suggested by the inability of the AHS model to capture the low q data in the concentrated systems. A model that incorporates some degree of softness in the repulsion and perhaps the charged nature of the corona could improve the interpretation of the data, particularly at low q.

The authors thank the Rhodia Complex Fluids Laboratory for the donation of materials and for financial support of portions of this work. The authors also thank Jyotsana Lal at IPNS, for her assistance in the neutron scattering measurements. This study benefited from the use of IPNS beam lines at Argonne National Laboratory, which are funded by the Office of Basic Energy Sciences, U.S. Department of Energy. This work was also supported in part by the National Science Foundation through the University of Massachusetts Materials Research Science and Engineering Center (MRSEC), award number DMR-0213695.

References

1. Cameron, N. S.; Corbierre, M. K.; Eisenberg, A. Can J Chem 1999, 77, 1311.
2. Zhang, L. F.; Eisenberg, A. Science 1995, 268, 1728.
3. Astafieva, I.; Zhong, X. F.; Eisenberg, A. Macromolecules 1993, 26, 7339.
4. Astafieva, I.; Khougaz, K.; Eisenberg, A. Macromolecules 1995, 28, 7127.

5. Groenewegen, W.; Egelhaaf, S. U.; Lapp, A.; van der Maarel, J. R. C. Macromolecules 2000, 33, 3283.
6. Groenewegen, W.; Lapp, A.; Egelhaaf, S. U.; van der Maarel, J. R. C. Macromolecules 2000, 33, 4080.
7. Tsitsilianis, C.; Iliopoulos, I. Macromolecules 2002, 35, 3662.
8. Bhatia, S. R.; Mourchid, A.; Joanicot, M. Curr Opin Colloid Interface Sci 2001, 6, 471.
9. Bhatia, S. R.; Crichton, M.; Mourchid, A.; Prud'homme, R. K.; Lal, J. Polym Prep 2001, 42, 326.
10. Bhatia, S. R.; Mourchid, A. Langmuir 2002, 18, 6469.
11. Bendejacq, D.; Ponsinet, V.; Joanicot, M.; Loo, Y. L.; Register, R. A. Macromolecules 2002, 35, 6645.
12. Charmot, D.; Corpart, P.; Adam, H.; Zard, S. Z.; Biadatti, T.; Bouhadir, G. Macromol Symp 2000, 150, 23.
13. Destarac, M.; Charmot, D.; Franck, X.; Zard, S. Z. Macromol Rapid Commun 2000, 21, 1035.
14. Krause, S.; Iskandar, M.; Iqbal, M. Macromolecules 1982, 15, 105.
15. Förster, S.; Burger, C. Macromolecules 1998, 31, 879.
16. Förster, S.; Hermsdorf, N.; Bottcher, C.; Lindner, P. Macromolecules 2002, 35, 4096.
17. Higgins, J. S.; Benoît, H. Polymers and Neutron Scattering; Clarendon: Oxford, England, 1994.
18. Goldmints, I.; vonGottberg, F. K.; Smith, K. A.; Hatton, T. A. Langmuir 1997, 13, 3659.
19. Yang, L.; Alexandridis, P.; Steytler, D. C.; Kositza, M. J.; Holzwarth, J. F. Langmuir 2000, 16, 8555.
20. Pedersen, J. S. Adv Colloid Interface Sci 1997, 70, 171.
21. Baxter, R. J. J Chem Phys 1968, 49, 2770.
22. Pham, Q. T.; Russel, W. B.; Thibeault, J. C.; Lau, W. Macromolecules 1999, 32, 2996.
23. Mellema, M.; Leermakers, F. A. M.; de Kruif, C. G. Langmuir 1999, 15, 6304.
24. Lobry, L.; Micali, N.; Mallamace, F.; Liao, C.; Chen, S. H. Phys Rev E 1999, 60, 7076.
25. Kotlarchyk, M.; Chen, S. H.; Huang, J. S.; Kim, M. W. Phys Rev A 1984, 29, 2054.
26. Prudhomme, R. K.; Wu, G. W.; Schneider, D. K. Langmuir 1996, 12, 4651.
27. Hamley, I. W.; Daniel, C.; Mingvanish, W.; Mai, S. M.; Booth, C.; Messe, L.; Ryan, A. J. Langmuir 2000, 16, 2508.
28. Bergenholtz, J.; Fuchs, M. Phys Rev E 1999, 59, 5706.
29. Lindman, B.; Alexandridis, P. Amphiphilic Block Copolymers: Self-Assembly and Applications; Elsevier: Amsterdam, 2000.